JOURNAL OF MATERIALS SCIENCE 14 (1979) 2163–2171

Stress-relaxation technique for deformation studies in four-point bend tests: application to polycrystalline ceramics at elevated temperatures

D. K. SHETTY, R. S. GORDON
Department of Materials Science and Engineering, University of Utah, Salt Lake City, Utah 84112, USA

The advantages of the stress-relaxation technique can be effectively realized by applying the procedure to conventional four-point bend tests usually employed in the deformation studies of ceramic materials. A test system and procedure for determining plastic strain rate–stress relationships at elevated temperatures (up to 1600° C) by the stress-relaxation method is described. An analysis to calculate true plastic strains and stresses from measured deflections and loads is presented and it is shown that such an analysis requires minimum assumptions regarding the materials behaviour. Preliminary results obtained on an iron-doped MgO specimen are discussed and compared with the constant load test results obtained on identical specimens. Sources of error in the four-point bend stress-relaxation tests and the methods to minimize them are also discussed.

1. Introduction

The stress-relaxation technique has long been used in the plastic deformation studies of metallic materials [1–3]. In recent years there has been a renewed interest in using this technique as a tool for establishing constitutive relations for inelastic deformations of metals and alloys [4]. Although the stress-relaxation technique has mostly been used in the conventional tension tests to determine plastic strain rate–stress relationships in metallic materials, the general principles of the technique have been applied in other tests. Thus, for example, subcritical crack-growth rates in brittle materials can be determined by a load-relaxation technique using fracture mechanics specimens such as double torsion specimens [5] or double cantilever beam specimens [6].

In the case of ceramic materials, specimen fabrication and testing difficulties generally do not permit tension tests to be used in deformation studies. Thin beam bend specimens have been used instead in constant load creep tests [7] and constant deflection rate tests [8] at elevated temperatures. Only limited attempts have been made to adapt the stress-relaxation technique to the bend test [9, 10]. The relaxation test procedure when applied to the four-point bend test has several advantages over the more conventional bend tests. (1) The relationship between stress and plastic strain rate can be established over wide ranges of stress (0.1 to 100 $MN m^{-2}$) and strain rates (10^{-3} to 10^{-9} sec^{-1}) in a single test. (2) By using a "stiff machine" one can minimize the total plastic strain accumulated in a relaxation test. Thus the stress–strain relationships are established at nearly constant plastic strain or at a state of constant "hardness" [11] in the test material. Repetition of stress-relaxation cycles then yields the effects of strain-hardening or plastic strain history on the stress–strain rate relationships. (3) Stress relaxation provides a means of studying deformation behaviour at high stress levels without the specimen undergoing large deflections so that the assumption regarding small deflections usually made in the bending

0022–2461/79/092163–09 $02.90/0

analysis is not violated. (4) It will be evident from the analysis presented in Section 3 that stress relaxation is one of the unique bend tests where outer fibre strains in the beam can be determined purely from geometric considerations. It eliminates *a priori* assumptions regarding the plastic behaviour of the material in the calculations of strains and stresses.

This paper describes a stress-relaxation test system (Section 2) designed to study the deformation behaviour of ceramic materials at elevated temperatures (up to 1600° C) using the thin beam four-point loading bend test geometry. An analysis to determine true plastic strains and stresses from the measured deflections and loads is presented in Section 3. Section 4 discusses preliminary results obtained on an iron-doped MgO specimen and compares the strain rate–stress results with the dead load creep data obtained on identical specimens. Sources of error in the four-point bend stress-relaxation tests are also discussed.

2. Stress-relaxation system and test procedure

In any stress-relaxation test, a specimen of defined geometry is loaded usually at a constant deflection rate to a predetermined load or deflection and then the total deflection is held constant. The specimen continues to deform plastically while the elastic deflection and hence the load drops with time in order to maintain total deflection constant. The rate of load drop, (dP/dt), is related to the plastic deflection rate, $\dot{Y}$, of the specimen through the total elastic compliance of the system, C, including specimen and the machine components such as load cell.

$$\dot{Y} = -C\left(\frac{dP}{dt}\right). \qquad (1)$$

The deflection rate, $\dot{Y}$, and the instantaneous load, P, are then converted to plastic strain rate and stress, respectively, using the specimen geometry and loading arrangement. The success of the stress-relaxation technique is critically dependent upon the temperature stability of the test system. Even small fluctuations in temperatures can affect the compliance, C, of the test system and can lead to load fluctuations that would limit the minimum plastic deflection rates that can be measured by the technique. The temperature stability requirements are particularly severe in the case of ceramic materials which are normally tested at elevated temperatures (1000 to 1750° C) and the specimen compliances are small.

2.1. Stress-relaxation system

Fig. 1 shows a schematic cross-sectional view of a stress-relaxation test assembly that is designed to test four-point bend specimens at temperatures up to 1600° C. The whole system is designed to be interfaced with the loading frame of a universal testing machine such as Instron Universal Testing Instrument model 1125. The system consists of three major components:

(1) high-temperature furnace/temperature control system;

(2) four-point loading system;

(3) centre-point deflection measuring system.

2.1.1. High-temperature furnace/ temperature control system

The design and construction of the furnace for the stress-relaxation system is indicated in Fig. 1. The furnace features Mo metal wire heating element and a light, all alumina, fibrous insulation in the interior. This makes the furnace lightweight for ease of mounting on the Instron frame. The exterior of the furance is constructed out of brass and is water-cooled on all surfaces. This eliminates heat flow to the Instron drive screw

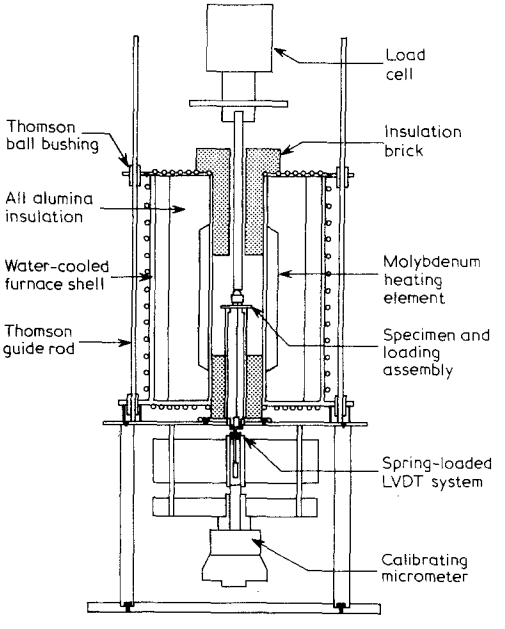

Figure 1 A schematic cross-sectional view of the stress-relaxation test assembly.

and hence load fluctuations. Four Thomson ball bushings are mounted on the furnace end plates. These enable the furnace to be moved up and down on guiding Thomson rods and facilitate access to the interior of the furnace for purposes of specimen mounting. The guide rods positioning the furnace are mounted on a stainless steel table below which is located the centre-point deflection measuring system. Two machined high-temperature insulation bricks (K 3000) cut down heat losses at the ends of the furnace tube. A purified H_2 gas atmosphere is maintained inside the furnace chamber during its operation.

A temperature controller–power supply unit (Research Incorporated Thermac Model: 625) allows temperatures to be controlled in the range 1000 to 1750° C with a maximum fluctuation no grater than ±0.25° C. Pt–Pt + 10% Rh thermocouples are used both to control and monitor the temperature. The useful lower limit of stress-relaxation rates obtained in this system are determined by the room-temperature fluctuations rather than the furnace-temperature variations.

2.1.2. Four-point loading system

The four-point loading system consists of accurately machined high density, recrystallized alumina rods for loading and a thick walled tube for supporting the specimen. Typical thin beam specimen dimensions are 1.25 mm × 4 mm × 30 mm. Single-crystal sapphire rods are used as support points and loading points on the specimen. A sapphire sphere is used to transmit the load to the specimen through a loading piece. The spherical contact point eliminates non-axial forces being transmitted to the specimen. The top loading rod is connected to a load cell mounted on the moving cross-head of the Instron machine through a water-cooled brass adaptor.

2.1.3. Centre-point deflection measuring system

It will be evident from the discussion in the following section that a continuous measurement of the deflection of the thin beam specimen at the centre point is essential for the determination of the bending strain from purely geometric considerations. The centre-point deflection is measured using a linear variable differential transformer (Schaevitz HR-DC 050). The body of the LVDT is mounted in an aluminium plate using a non-conductive grade LE phenolic mount. The aluminium plate is fitted with ball bushings and is movable along Thomson guide rods. A non-rotating spindle micrometer, with a measurement sensitivity of 2×10^{-5} in., is used for both calibrating the LVDT and positioning the LVDT body for desired initial output. The LVDT core is connected through a threaded core connector to an alumina rod that acts as a deflection measuring probe. The core assembly is spring-loaded so as to ensure continuous contact of the probe tip with the lower face of the specimen. A ball bushing in the centre of the stainless steel table maintains the axiality of the deflection measuring core assembly.

2.2. Test procedure

The relaxation test procedure involves rapid loading of the bend specimen to a desired initial load at a constant deflection rate. The initial deflection rate for loading, which determines the maximum deformation rate of the bend specimen, is selected to be compatible with the load-recording response of the test machine. At the preselected load the cross-head is arrested and the load and the centre-point deflection are continually recorded until the minimum relaxation rates characteristic to the system are attained. A typical load and centre-point deflection recording obtained in a relaxation test on an iron-doped MgO specimen at 1450° C is shown in Fig. 2. In the stress-relaxation test system described here meaningful strain (creep) rates in the range 10^{-3} to 10^{-9} sec^{-1} can be obtained in a good test.

3. Analyses of stresses and strains in relaxation tests in four-point bend specimens

A rigorous analysis of stresses and strains in a four-point bend test specimen under plastic deformation conditions is a complex problem. This complexity is due to the fact that a bend specimen is a composite of a large number of fibres subjected to different deformation conditions and the externally measured loads and deflections are complex resultants of the stresses and strains of the individual fibres. A number of assumptions are usually made to make the bend specimen amenable to analysis. The following assumptions, which are inherent to the well-known elastic bending analysis, are also made here [12].

(1) Plane cross-sections before bending remain plane after bending; in other words, the strain

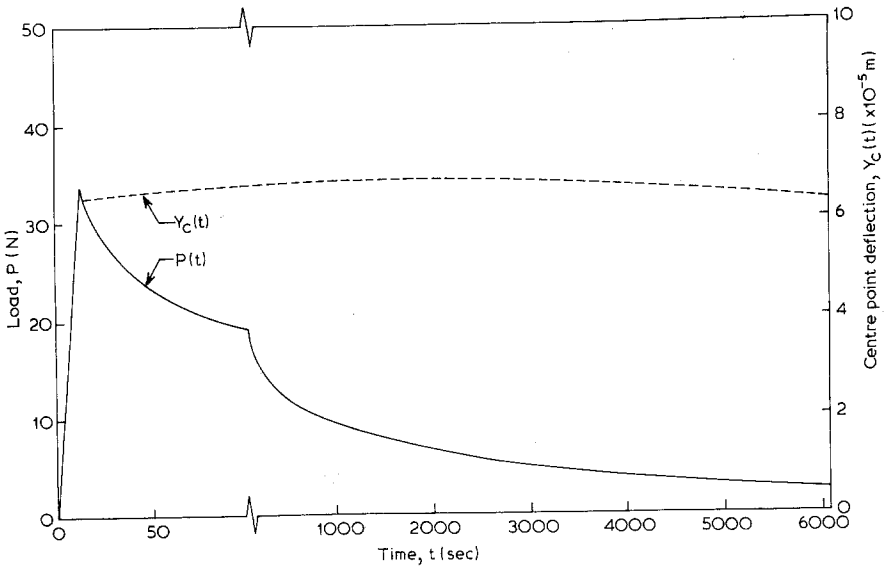

Figure 2 Typical load-relaxation and centre point deflection plots obtained for an (MgO + 0.53% Fe) specimen at 1450° C.

at a point in a given cross-section varies linearly with its distance from the neutral axis.

(2) The analysis is limited to beams that are long compared with their cross-sectional dimensions. In this case shear deflections can be neglected.

(3) Bending displacements are small compared with the length of the beam.

(4) The plastic behaviour of the material in tension and compression are identical except for sign.

Using the above four assumptions the maximum plastic strain and stress in the outer fibre of a four-point bend specimen can be determined in the following manner.

3.1. Calculation of maximum plastic strain

In a four-point bend specimen the bending moment, M, and therefore the curvature of the plastically bent beam is constant along the span between the two inner load points as indicated in Fig. 3. Then it can be shown [13] that for small deflections, i.e. $a \gg Y_r$,

$$\epsilon_{max} = \frac{4h}{a^2} Y_r = \frac{4h}{a^2} (Y_c - Y_L) \qquad (2)$$

where ϵ_{max} is the maximum plastic strain in the outer fibre, Y_c the plastic deflection at the centre of the beam, Y_L the plastic deflection at the load points, h the thickness of the beam, and a the distance between load points. The plastic deflections, Y_c and Y_L, can be obtained from the centre-point deflection and load records of Fig. 2.

$$Y_c = Y_{c0} + [Y_c(t) - P(t) \cdot C_c] \qquad (3)$$

where Y_{c0} is the plastic deflection of the centre-point prior to the stress-relaxation test, $Y_c(t)$ is the total centre-point deflection at any time, t (Fig. 2), $P(t)$ is the corresponding load at time, t, and C_c the elastic centre-point compliance.

$$Y_L = Y_{L0} + C_L \cdot [P(0) - P(t)] \qquad (4)$$

where Y_{L0} is the plastic deflection of the load point prior to the stress-relaxation test, $P(0)$ is the initial maximum load during the stress-relaxation test, and C_L the elastic load point compliance.

The elastic compliances, C_c and C_L, can be determined from the slopes of the initial loading

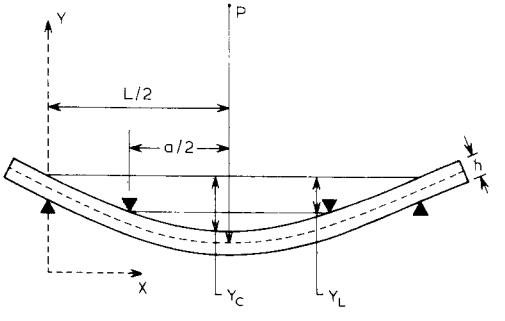

Figure 3 The geometrical parameters for a deformed four-point bend specimen.

parts of the load–time and centre-point deflection–time plots of Fig. 2 and the cross-head speed used for initial loading. If these initial loading sections of the plots are non-linear the maximum slopes are taken to determine C_c and C_L and the accompanying plastic deflection is included in Y_{c0} and Y_{L0}. It may be noted that the load point compliance, C_L, is calculated using the cross-head speed and hence it is a total compliance including the machine compliance, C_m. The centre-point compliance, C_c, on the other hand, is based on direct deflection measurement on the specimen and hence should correspond to the theoretical value from elastic analysis. It is clear from the strain analysis presented here that one requires deflection measurements at both load point and centre point to determine the curvature and hence maximum plasic strain. In most bend tests it is difficult to experimentally measure deflections at both of these points. Stress relaxation, on the other hand, allows a direct measurement of centre-point deflection and an indirect measurement of load-point deflection thus enabling one to make strain calculation from purely geometric considerations.

3.2. Calculation of maximum outer fibre stress

For materials that exhibit a unique steady state creep law such as the general power creep relation

$$\dot{\epsilon} = A\sigma^N \tag{5}$$

where the stress exponent, N, is independent of stress, it can be shown [12, 13] that the maximum outer fibre stress in a four-point bend specimen is given by the relation

$$\sigma_{max} = \left(\frac{Mh}{2I}\right)\left(\frac{2N+1}{3N}\right) \tag{6}$$

where M is the bending moment in the inner span, and I is the moment of inertia of the cross-section. It can also be shown [12] for this case that the stress exponent, N, can be determined from the measured steady-state deflection rates such as centre-point deflection rates, $\dot{Y}_c$, and the applied loads, P, from a log–log relation

$$\text{Log } \dot{Y}_c = N \log P + C. \tag{7}$$

Once N is determined, the maximum stress is calculated from Equation 6 and the corresponding maximum creep strain, ϵ_{max}, is obtained from the measured centre-point deflection and the value of N:

$$\epsilon_{max} = \left(\frac{4h(N+2)}{2L(L+aN)-Na^2}\right)Y_c. \tag{8}$$

It may be noted that for the special case $N = 1$, i.e. viscous creep law, both Equations 6 and 8 reduce to the well-known expressions for stress and strain obtained in the elastic bending analysis.

Real materials, however, do not exhibit a unique power law creep behaviour (Equation 5) at all stress levels. In general, N is a function of stress and, in particular, for many materials the creep law changes from a viscous creep law ($N = 1$) at low stresses to a power creep law at high stresses [14]. The maximum stress in the bend specimen of these materials with the general creep behaviour can still be determined, however, by using an analysis suggested by Bilde-Sörensen [15]. In this analysis the only requirement with respect to the material creep behaviour is that the steady-state creep rate, $\dot{\epsilon}$, be a continuously increasing function of the stress, σ, and equal to zero for $\sigma = 0$ [15]. Then it is shown that the maximum stress in the bend specimen is still given by a relation similar to Equation 6.

$$\sigma_{max} = \left(\frac{Mh}{2I}\right)\left(\frac{2N'+1}{3N'}\right) \tag{9}$$

where the exponent, N', is defined as

$$N' = \text{d log } \dot{\epsilon}_{max}/\text{d log } M. \tag{10}$$

The stress analysis described by Equations 9 and 10 is particularly useful in stress-relaxation tests where applied load (and therefore bending moment) is measured as a function of the deflection rates of the load points and the centre point (Equations 3 and 4). These measured deflection rates can be converted to strain rates using only the geometrical relation, Equation 2. The moment exponent, N', and therefore, σ_{max} can then be calculated at different applied loads. Thus the procedure described here permits the calculation of maximum strain rates and maximum stresses in a four-point bend specimen deforming in a steady-state manner without making assumptions *a priori* regarding its creep behaviour.

4. Discussion

The analysis for strains and stresses in a four-point bend specimen undergoing steady-state

plastic deformation discussed in Section 3 was applied to a typical stress-relaxation test data such as shown in Fig. 2. This test was conducted on a 43 μm grain size $MgO-Fe_2O_3$ solid solution specimen with 0.53 cation % Fe at 1450° C. This material was chosen because of the extensive dead load creep data available for comparison purposes [7, 16, 17]. The stresses and strain rates were calculated from load and deflection data by numerical methods using a computer.

The creep rate–stress relation analysed from the stress-relaxation test data of Fig. 2 is shown in Fig. 4. For comparison purposes the stress-relaxation data were also analysed using equations of elastic bending analysis (Equations 6 and 8 with $N = 1$) based on centre-point deflection. Several interesting features can be noted in the creep rate–stress plots of Fig. 4. There is a well-defined transition in creep behaviour; in the low stress regime the creep behaviour is characterized by a low stress exponent N in the creep law ($N = 1.77$) and above a transition stress the stress exponent increases to 4.12. In dead load creep studies in identical composition specimens, stress exponents of 1.0 (at 1425° C, grain size 65 μm) [16] and 3.4 (at 1500° C, grain size 258 μm) [18] have been observed in the low and high stress regimes, respectively. The reasons for these differences in the observed stress exponents in the two types of tests are not yet clear and additional experiments are currently underway to verify these differences. The second feature of the results in Fig. 4 is the difference in the creep rate–stress results obtained by the two analyses. In the low stress regime the two analyses yield nearly identical creep rates and stresses. In the higher stress regime there is substantial difference in the results of the two analyses and this difference is primarily due to the over-estimation of the stress in the elastic analysis by assuming $N = 1$ in Equation 6.

As pointed out by Bilde-Sörensen, the moment exponent, N', in general is not equal to the stress exponent N. The two exponents are identical only when there is a unique creep law with the stress exponent N being independent of stress. The difference between the two exponents can be illustrated for general creep behaviour (N is a function of stress) by using a numerical procedure to determine the stress profile across the thickness of the bend specimen. This is demonstrated in the Appendix for the special situation of transition creep behaviour where the power creep law changes abruptly with a change in the stress exponent N at the transition stress (Fig. 5). The corresponding stress profiles in the bend specimen and the difference between stress and moment exponents are illustrated in Fig. 6 and 7, respectively.

Although the analysis presented in Section 3 for the maximum stresses and strains in a plastic-

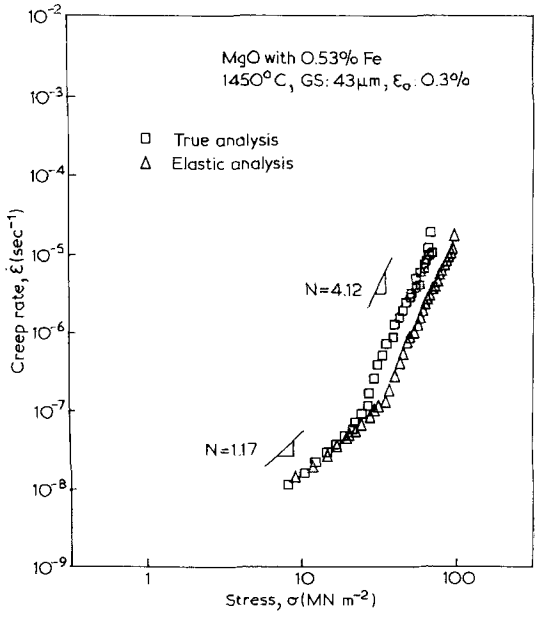

Figure 4 Creep rate–stress results analysed from the stress-relaxation test data of Fig. 2.

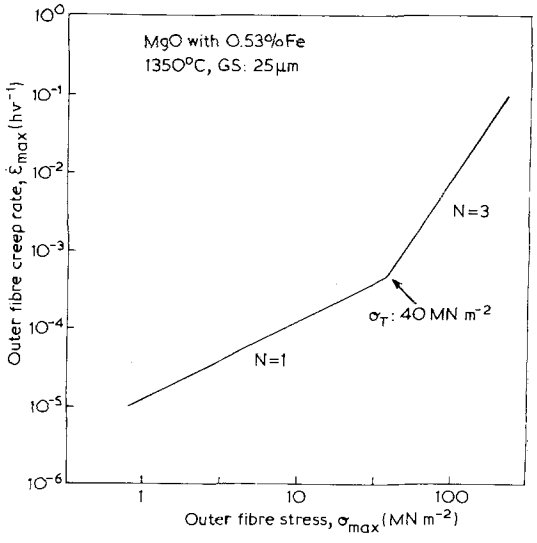

Figure 5 Viscous-power law transition creep behaviour predicted for (MgO + 0.53% Fe) specimen at 1350° C and grain size 25 μm.

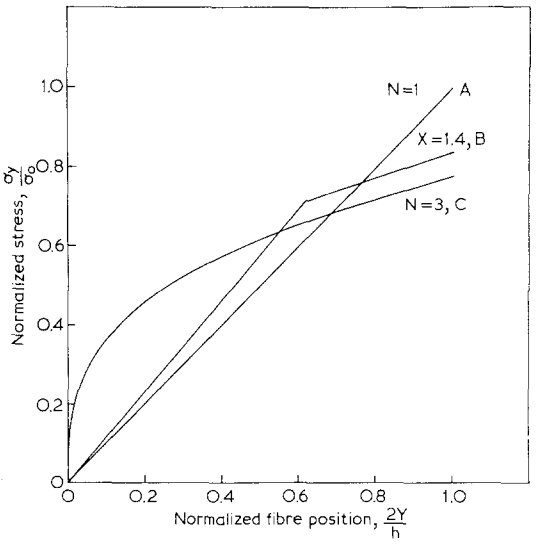

Figure 6 The stress distribution profile across the thickness of a bend specimen obeying transition creep behaviour (curve B).

ally deforming four-point bend specimen is the most general one, two assumptions regarding the material creep behaviour are still implicit in this analysis. The first assumption is with respect to the creep behaviour of the material in tension and compression. They are assumed to be identical. This is equivalent to assuming the neutral axis of the beam to be at the centre of the cross-section. It is difficult to evaluate the applicability of this assumption particularly in ceramics where comparative experiments in tension and compression are lacking. Secondly, the analysis assumes steady-state creep behaviour where the creep rate is independent of strain. If the deformation is transient in nature or strain-hardening effects decrease creep rates with increasing creep strain, then an additional correction incorporating a strain-hardening exponent must be made to evaluate the stress [8]. This correction, however, is not too significant in stress-relaxation bend tests since a very small amount of strain is accumulated in each stress-relaxation cycle and one obtains creep rate–stress data at approximately constant strain.

The major source of error in evaluating creep behaviour of materials from stress-relaxation bend tests is in the calculation of the load-point deflection, Y_L, from the magnitude of relaxed load $[P(0)-P(t)]$ in Equation 4. Local deformation at the sapphire load points and extraneous load relaxation due to the same tend to over-estimate both C_L and $[P(0)-P(t)]$ from pure bending. This leads to an under-estimate of the maximum strain in Equation 2. This error in the strain and hence strain-rate calculation can be minimized in the following ways. The inner loading span length, a, should be a reasonably large fraction of the support span length, L. This tends to increase Y_c relative to Y_L and hence decreases the effects of error in Y_L on the strain. Secondly, the specimen compliance must be increased by reducing thickness so that deflections due to bending are very much greater then localized load-point deformations. Finally, the localized deformations at load points tend to decrease with repeated stress-relaxation cycles. The load-point compliance, C_L, should therefore, be determined from its saturated value. The simultaneous measurement of the centre-point deflection during a stress-relaxation test provides an indication of the extent of the extraneous relaxations. In an ideal stress-relaxation bend experiment the centre-point deflection, after the initial loading, should always increase with decreasing slopes, but in actual stress-relaxation tests the centre-point deflection decreases slightly after an initial increasing period. This indicates the occurrence of extraneous relaxations and if the rate of decrease of centre-point deflection, $(-dY_c(t)/dt)$, approaches the elastic contraction rate $(C_c \cdot dP(t)/dt)$, it indicates the point when all the load relaxations are due to extraneous factors and not due to the plastic bending of the beam.

5. Conclusions

The stress-relaxation test procedure can be use-

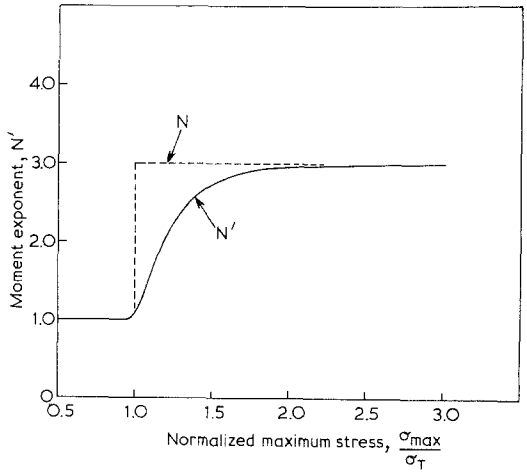

Figure 7 A comparison of stress exponent N and moment exponent N' for bend specimens obeying transition creep behaviour.

fully applied to four-point bend tests in the deformation studies of ceramic materials at elevated temperatures. A simple analysis can be applied to evaluate true plastic strains and stresses from measured deflections and loads during a relaxation test. This analysis is applicable for any general steady-state deformation behaviour of material and does not require *a priori* assumption regarding the same. Preliminary results obtained on an iron-doped MgO specimen show reasonable agreement with constant load creep data obtained on the same material.

6. Appendix

The stress distribution in a four-point bend specimen obeying a general steady-state creep law can be determined by an iterative numerical procedure. This is demonstrated for the case of transition creep behaviour where a linear viscous creep law is obeyed for stresses below a transition stress, σ_T, and a power law holds good above σ_T.

$$\dot{\epsilon} = A \cdot \sigma^N \quad \text{for} \quad \sigma > \sigma_T \qquad \text{(A1)}$$

$$\dot{\epsilon} = B \cdot \sigma \quad \text{for} \quad \sigma < \sigma_T.$$

Such a creep behaviour predicted for an MgO + 0.53% Fe, specimen at 1350° C is indicated in Fig. 5 [19].

The strains and strain rates vary linearly across the thickness of the bend specimen.

$$\dot{\epsilon}(Y) = \dot{\epsilon}_{max} \cdot \frac{2Y}{h} \qquad \text{(A2)}$$

where Y is the distance from the neutral axis.

The stress distribution in the bend specimen should balance the external bending moment

$$M = 2b \int_0^{h/2} \sigma(Y) \cdot Y \cdot dY. \qquad \text{(A3)}$$

The stress distribution for any given external bending moment, M, is determined in the following manner. First a maximum stress at the outer fibre is assigned preferably the elastic stress value, σ_0, corresponding to the bending moment, M. The maximum strain rate corresponding to this stress us obtained from Equation A1. This, in turn, determines strain rates at every fibre of a large number of fibres across the thickness. These strain rates determine a stress distribution according to Equation A1 from which an internal resisting bending moment is calculated by numerical integration using Equation A3. If the calculated bending moment is greater then the external bending moment, a new outer fibre stress, $(\sigma_0 - \Delta\sigma)$, is assumed and the sequence of calculation repeated. This iteration procedure is repeated until the internal bending moment balances the external bending moment. The accuracy of the calculation is determined by the decrement in stress, $\Delta\sigma$.

The stress distribution determined in this manner for the transition creep behaviour is shown in Fig. 6 (curve B) where X is defined by the ratio (σ_0/σ_T). The elastic stress distribution (curve A) and power law stress distribution (curve C) are also indicated in Fig. 6.

The above procedure for calculating stresses and internal bending moment can now be repeated to generate the functional relation

$$\dot{\epsilon}_{max} = F(M). \qquad \text{(A4)}$$

From this one can obtain the moment exponent

$$N' = d \log \dot{\epsilon}_{max} / d \log M. \qquad \text{(A5)}$$

A plot of N' as a function of the maximum stress for the transition creep behaviour is shown in Fig. 7. For stresses greater than the transition stress, σ_T, N' is less than N and it approaches N asymptotically.

Acknowledgements

The authors are grateful for helpful discussions with Dr A. V. Virkar. This research was supported by the Department of Energy contract no EY-76-S-02-1591.*002.

References

1. P. FELTHAM, *Phil. Mag.* **6** (1961) 259.
2. F. GUIU and P. L. PRATT, *Phys. Stat. Sol* **6** (1964) 3.
3. D. LEE and E. W. HART, *Met. Trans.* **2** (1971) 1245.
4. E. W. HART, C. -Y. LI, H. YAMADA and G. L. WIRE, in "Constitutive equations in Plasticity", edited by A. S. Argon (MIT Press, Cambridge, Mass, (1975).
5. D. P. WILLIAMS and A. G. EVANS, *J. Test. Eval.* **1** (1973) 264.
6. A. V. VIRKAR and R. S. GORDON, *J. Amer. Ceram. Soc.* **59** (1976) 68.
7. G. R. TERWILLIGER, H. K. BOWEN and R. S. GORDON, *ibid* **53** (1970) 241.
8. A. H. HEUR, R. M. CANNON and N. J. TIGHE, in "Ultrafine-Grain Ceramics", edited by J. J. Burke, N. L. Reed and V. Weiss (Syracuse University Press, Syracuse, New York, 1970) p. 339.

9. J. T. A. ROBERTS, *Acta Met.* **22** (1974) 873.
10. P. A. LESSING, Ph.D. Thesis, University of Utah (1976).
11. E. W. HART, *Acta Met.* **18** (1970) 599.
12. I. FINNIE and W. R. HELLER, "Creep of Engineering Materials" (McGraw-Hill, New York, 1959) pp. 135–7.
13. G. W. HOLLENBERG, G. R. TERWILLIGER and R. S. GORDON, *J. Amer. Ceram. Soc.* **54** (1971) 196.
14. A. G. EVANS and T. G. LANGDON, *Prog. Mat. Sci.* **21** (1976) 386.
15. J. B. BILDE-SÖRENSEN, *J. Amer. Ceram. Soc.* **58** (1975) 70.
16. R. T. TREMPER, R. A. GIDDINGS, J. D. HODGE and R. S. GORDON *ibid* **57** (1974) 421.
17. R. S. GORDON and J. D. HODGE, *J. Mater. Sci.* **10** (1975) 200.
18. P. A. LESSING and R. S. GORDON, in "Deformation in Ceramic Materials", edited by R. C. Bradt and R. E. Tressler (Plenum Press, New York, 1975) 271.
19. J. D. HODGE, P. A. LESSING and R. S. GORDON, *J. Mater. Sci.* **12** (1977) 159.

Received 3 November 1978 and accepted 22 January 1979.